Nonlinear Speed Controller Supported by Direct Torque Control Algorithm and Space Vector Modulation for Induction Motors in Electrical Vehicles

I. Aliskan[1], K. Gulez[2], G. Tuna[3], T. V. Mumcu[2], Y. Altun[2]
[1]*Department of Electrical and Electronics Engineering, Bulent Ecevit University, Zonguldak, Turkey*
[2]*Department of Control and Automation Engineering, Yildiz Technical University, 34220, Istanbul, Turkey*
[3]*Department of Computer Programming, Edirne Vocational School of Technical Sciences, Trakya University, Edirne, Turkey*
gurkantuna@trakya.edu.tr

***Abstract*—Energy mode functions and their inverse signal dynamics can be used for the design of controllers in classical control algorithms, which use the error signals of related system parameters in general mode. Different from this common approach, Lyapunov function-based controller design is preferred and motor mechanical speed parameter is incorporated into the control operation in this study. The results of the experimental studies conducted for this study prove that when both electrical and mechanical parameters of the system are taken into consideration, the proposed controller, nonlinear speed controller supported by direct torque controller and space vector modulation, performs better than classical controllers and can be realized successfully.**

***Index Terms*—Nonlinear speed controller, induction motor, direct torque control, space vector modulation.**

I. INTRODUCTION

Direct torque control algorithms for induction motors use reference torque values. Therefore, the transformation of reference speed values into reference torque values is needed. Classical feedback controllers use speed error values for the transformation. In addition, different system parameters are incorporated into the transformation for a better control operation [1], [2]. As it is well-known, resolution is important for controller calculations and frequency is important at time sharing switching operations [3], [4].

In this study, starting from the design of Lyapunov function-based nonlinear controller, mechanical speed value and speed error value are used for the control transformation. To obtain the required torque value, reference speed value is transformed by either classical speed control or nonlinear speed control methods. In this study, PI controller is preferred for the classical speed control and reference controller is obtained by using well-known Ziegler-Nichols tuning rule. Unit step function is used for input reference at design operation [5]. For the nonlinear speed control, Lyapunov function-based nonlinear controller is proposed. The design of the proposed controller is based on an energy function and opposite signed dynamics of this function. Zero is fixity point for the functions [6], [7]. In addition, a parameter of the controlled system is used in the energy functions and the dynamic functions. Pause point is expected to be almost 1 for the control parameters. The torque controller uses a reference value provided to the controller. A gas pedal is used to set a reference speed value. The speed controller transforms the speed value into the reference torque value. The torque controller calculates required voltage vector for the motor and sends the vector to inverter controller. For the motor system, a power electronic inverter is used to invert direct currents to alternative currents. Time sharing-based vector controller sets the required voltage vector. Angular and amplitude values of the vector are obtained by the inverter control system. For experimental evaluations in this study, a rotational loaded system was used. In the design steps, the variation of electromagnetic torque parameter was taken into consideration. Required reference torque was created by using the reference speed value for direct torque controller (DTC).

Manuscript received June 24, 2012; accepted April 19, 2013.

II. DIRECT TORQUE CONTROL

Induction machine model is described in the general reference frame by using the following equations:

$$\overline{V}_s^g = R_s \cdot \overline{i}_s^g + \frac{d\overline{\psi}_s^g}{dt} + j \cdot \omega_g \cdot \overline{\psi}_s^g , \quad (1)$$

$$0 = R_r \cdot \overline{i}_r^g + \frac{d\overline{\psi}_r^g}{dt} + j(\omega_g - \omega_r)\overline{\psi}_r^g , \quad (2)$$

$$\overline{\psi}_s^g = L_s \cdot \bar{i}_s^g + L_m \cdot \bar{i}_r^g , \quad (3)$$

$$\overline{\psi}_r^g = L_r \cdot \bar{i}_r^g + L_m \cdot \bar{i}_s^g , \quad (4)$$

where $\overline{V}_s$ is supply voltage signal of induction motor stator, $\bar{i}_s$ and $\bar{i}_r$ are stator and rotor currents, ω_g is general reference speed, ω_r is rotor angular velocity speed, R_s and R_r are stator and rotor resistances, $\overline{\psi}_s^g$ and $\overline{\psi}_r^g$ are stator and rotor field linkages. L_s represents the parameter of stator leakage inductance, L_r represents the parameter of rotor leakage inductance, and L_m represents the parameter of mutual inductance. The superscript "g" refers to reference frame [8], [9].

Mechanical dynamics of the induction motor is described as follows:

$$T_e = \frac{3}{2} \cdot \frac{p}{2} \cdot \mathrm{Im}\left(\overline{\psi}_s^g \cdot \bar{i}_s^g\right), \quad (5)$$

$$J \cdot \frac{d\omega_m}{dt} = J \cdot \frac{2}{p} \cdot \frac{d\omega_r}{dt} = T_e - T_{load} , \quad (6)$$

where T_e is the motor torque, p is the number of motor poles, J is system inertia, ω_m is rotor mechanical angular velocity speed, and T_{load} is load torque value [8]. One of the six non-zero and two zero voltage vectors is selected by the torque controller and required switch positions are sent to the inverter [10], [11]:

$$\Delta T_e = T_{e_{ref}} - T_e , \quad (7)$$

$$\Delta \psi_s^g = \overline{\psi}_{s_{ref}}^g - \overline{\psi}_s^g , \quad (8)$$

where ΔT_e and $\Delta \psi_s^g$ are the symbols of torque and flux errors, respectively. $T_{e_{ref}}$ and $\overline{\psi}_{s_{ref}}^g$ represent the reference values of T_e and $\overline{\psi}_s^g$, respectively. For selecting voltage vector, the errors must be taken into the hysteresis bands. The $\overline{V}_s^g$ vectors can be calculated using (9) [10]

$$\overline{V}_s^g = \frac{2}{3} \cdot V_{dc} \cdot \left(S_a + e^{j \cdot \frac{2.\pi}{3}} \cdot S_b + e^{j \cdot \frac{4.\pi}{3}} \cdot S_c \right), \quad (9)$$

where S_a, S_b and S_c represent stator phase A, phase B, and phase C, respectively.

When the vector is selected, stator flux is rotated to desired frequency, which is inside a specified band. If the motor stator ohmic drops are neglected, stator flux dynamic is calculated using (10)

$$d\overline{\psi}_s^g = \overline{V}_s^g \cdot \Delta t . \quad (10)$$

If (11) below and (5) are used together, a sinusoidal function of γ is obtained on motor torque. γ is the angle value between stator and rotor fields of induction motor. The angle is adapted and required stator field is obtained using (13) and (14), respectively [12]:

$$\bar{i}_s = \frac{\overline{\psi}_s^g}{\sigma L_s} - \frac{L_m}{\sigma L_s L_r} \overline{\psi}_r^{g'} \quad and \quad \sigma = 1 - \frac{L_m^2}{L_s L_r} , \quad (11)$$

$$T_e = \frac{3}{2} \frac{p}{2} \frac{L_m}{\sigma \cdot L_s \cdot L_r} \cdot \left|\overline{\psi}_s^g\right| \cdot \left|\overline{\psi}_r^{g'}\right| \cdot \sin\gamma , \quad (12)$$

$$\overline{\psi}_s^s = \int \left(\overline{V}_s^s - \bar{i}_s^s . R_s \right) dt , \quad (13)$$

$$T_e = \frac{3}{2} \cdot p \cdot \left(\psi_{ds}^s \cdot i_{qs}^s - \psi_{qs}^s \cdot i_{ds}^s \right), \quad (14)$$

where the superscript "s" refers to stator reference frame. ψ_{ds}^s is the real axis component of stator magnetic field space vector fixed coordinate system, ψ_{qs}^s is the imaginary axis component of stator magnetic field space vector fixed coordinate system, i_{ds} is the real axis of stator flux in the fixed coordinate system, and i_{qs} is the imaginary axis of stator flux in the fixed coordinate system.

Measured stator voltage and stator current signals are represented with $\overline{V}_s^s$ and $\bar{i}_s^s$. $\overline{\psi}_s^s$ represents calculated stator field vector. $\Delta\overline{\psi}_s^g$ and ΔT_e states are enough for voltage vector selection [9]. The details of the proposed control system and data flow in the proposed control system are shown in Fig. 1.

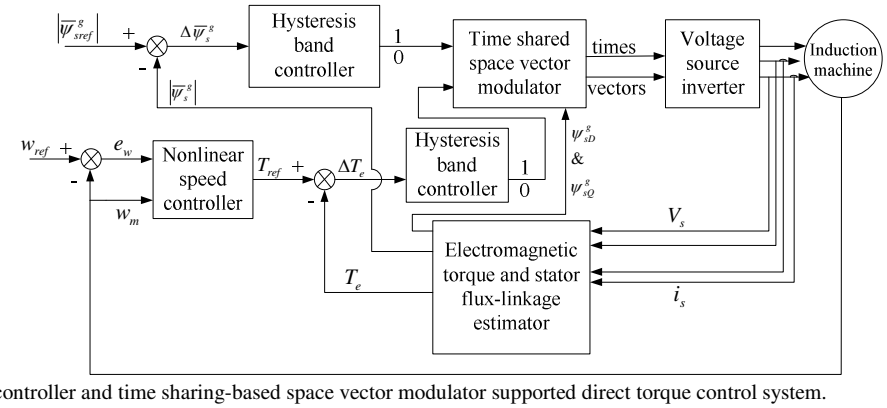

Fig. 1. Nonlinear speed controller and time sharing-based space vector modulator supported direct torque control system.

III. TIME SHARING-BASED SPACE VECTOR MODULATION

The disadvantage of classical direct torque control systems is the use of inverter control modulator. This disadvantage is reinforced with time sharing-based space vector modulator which supplies required voltage vector at angle position. The hysteresis band values and flux vector components are placed into the time sharing-based space vector modulator. Measured voltage and current parameters are used for the calculation of stator flux vector. These parameters are also used for the calculation of electromagnetic torque. Torque error value and flux vector positions on their hysteresis bands are enough for selecting required supply voltage vector [13], [14].

The position, stator flux band position and torque error band position are used in three different cases. In the first case, flux angular position ε_R :0°…60° is placed in the band area and both of the band values are positive. First active vector is selected as $\overline{V}_1$ and second active vector is selected as $\overline{V}_2$. $t_{vector\,number}$ is relevant vector switching time and t_{total} is total switching period. Then, ε_R is determined in 0°…360° circular area. When these parameters are used, following time parts are obtained:

$$\begin{cases} t_1 = t_{total}.\sin(60-\varepsilon_R)/\sin(60), \\ t_2 = t_{total}.\sin(\varepsilon_R)/\sin(60), \\ t_0 = t_7 = \left(t_{total} - t_1 - t_2\right)/2. \end{cases} \quad (15)$$

In the second case, ε_R :120°…180° is placed in the band area, the flux band value is positive and torque error band value is equal to zero. This means $t_1 = t_{total}$ and $t_2 = t_0 = t_7 = 0$ time values must be chosen in time domain. In the third case, torque error band value and stator flux band value have negative signs and ε_R :0°…60° angular position. Then, $\overline{V}_5$ and $\overline{V}_6$ active vectors are selected and switching time parts are calculated as follows

$$\begin{cases} t_5 = \dfrac{t_{total}.\left\{\sin(60-\varepsilon_R) - \left[\tan(240).\cos(240+\varepsilon_R)\right]\right\}}{\sin(300) - (\cos(300).\tan(240))}, \\ t_6 = t_{total}.\left\{\cos(240+\varepsilon_R)/\cos(240)\right\} - t_5.\left[\cos(300)/\cos(240)\right], \\ t_0 = t_7 = \left(t_{total} - t_5 - t_6\right)/2. \end{cases} \quad (16)$$

IV. PERFORMANCE EVALUATIONS

In the proposed system, nonlinear speed controller and time sharing-based space vector modulator are integrated into the induction motor control system. For experimental evaluations in this study, induction motor parameters, R_1=1.027 Ω, R_2=1.475 Ω, L_0=112.7 mH, $L_{\sigma 1} = L_{\sigma 2}$ = 8.07 mH and J=0.089 kg.m². DC supply voltage is 336 V.

To compare the proposed system with pulse width controlled system, time constant, 20 μs, and carrier frequency, 20 kHz, are used for discrete time applications with pulse width modulator controlled inverter in MATLAB. Sampling time, 50 μs, and t_{1total}=800 μs are used for discrete time application system with time sharing-based space vector modulator controlled inverter in MATLAB. Fig. 2 shows the values of the block parameters of insulated gate bipolar transistor (IGBT) inverter used in this study.

Due to the disadvantage that the PCI card added to the system together with the optoelectronic switches has only one analog to digital converter and one digital to analog converter, stator currents-voltages and encoder signals slide on time phase. Hence, in this system, desired performance characteristics may not be obtained by control algorithms.

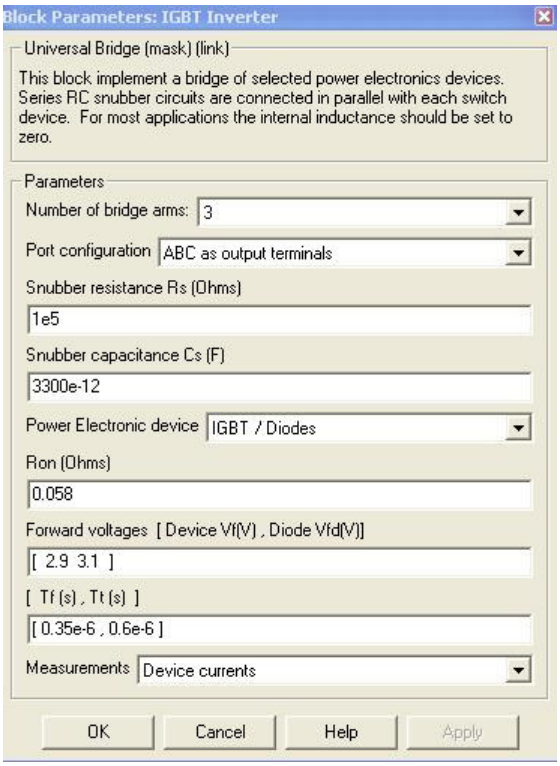

Fig. 2. Block parameters of the IGBT inverter.

Upper valued time parameters are used for pulse width modulator-based system. DC supply voltage is selected as 141 V for both systems. If voltage signals are taken into consideration, the result of the pulse modulator is 110-155 V and the result of the space modulator is 140±8 V. Desired sinusoidal current signal, $i_{continuous} = 2 \cdot \sin(2\pi \cdot 50 \cdot t)A$, is generated in the stator windings by the space vector modulator controlled inverter. As it is well-known, circular shaped flux is desired for the best performance of induction motors [1], [4]. Fig. 3 (a) and (b) show the results of stator phase-A voltage signals obtained from the pulse width modulator and the time shared space vector modulator, respectively.

Fig. 4 (a) and (b) show the results of stator phase-A current signals obtained from the pulse width modulator and the time shared space vector modulator, respectively. Fig. 5 (a) and (b) show the results of stator flux positions in D-Q axis obtained from the pulse width modulator and the time shared space vector modulator, respectively. It is seen that desired flux structure is formed by the space vector modulator. The reason of axis slidings is the PCI card used for analog to digital and digital to analog conversions.

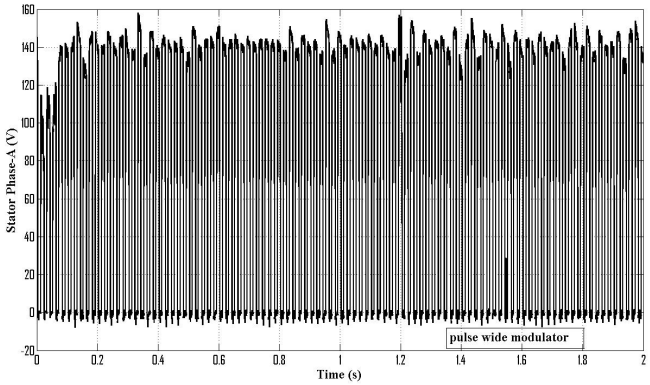

(a)

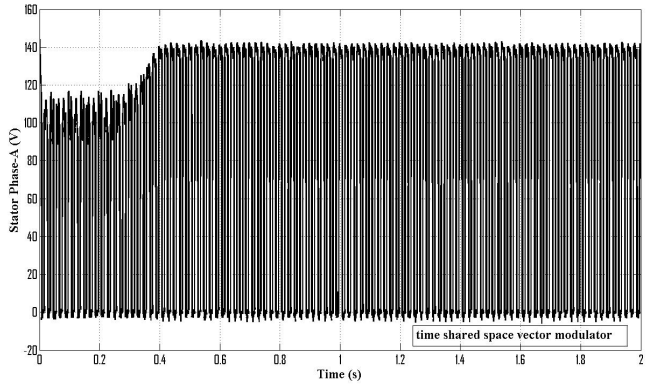

(b)

Fig. 3. Stator phase-A voltage signals time positions.

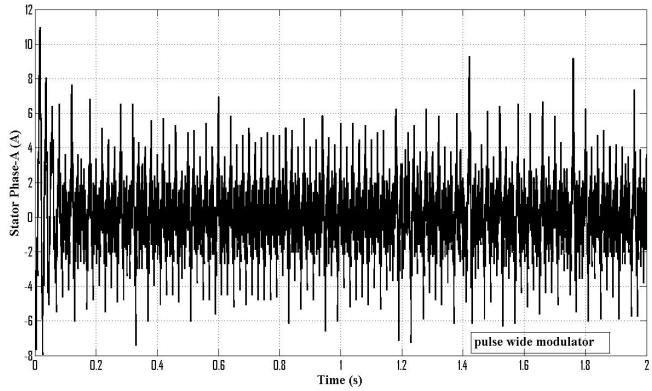

(a)

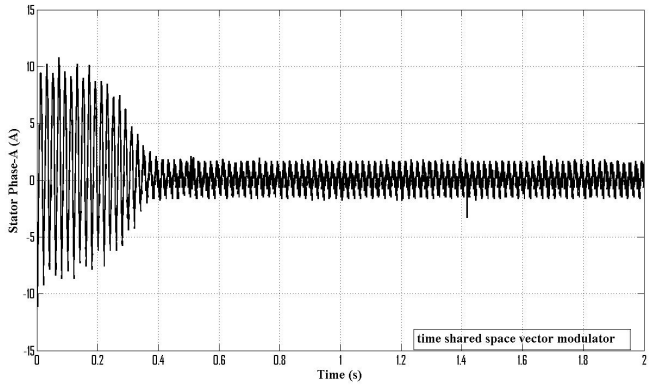

(b)

Fig. 4. Stator phase-A current signals time positions.

In Fig. 6 (a) and (b), the positions of rotor mechanical speeds in time domain obtained from the pulse width modulator and the time shared space vector modulator are shown. After 0.1 sec, pulse width controlled system takes its continuous time position. On the other hand, the proposed space vector controller is slower. It takes its continuous time position after 0.4 sec. But, ~±80rpm fluctuation of the pulse width controlled motor shows that its performance is worse in continuous time.

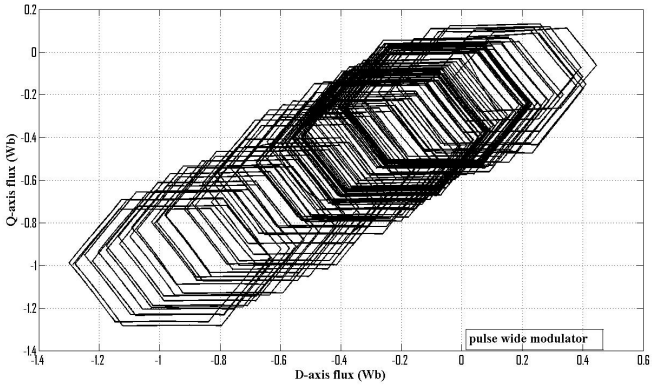

(a)

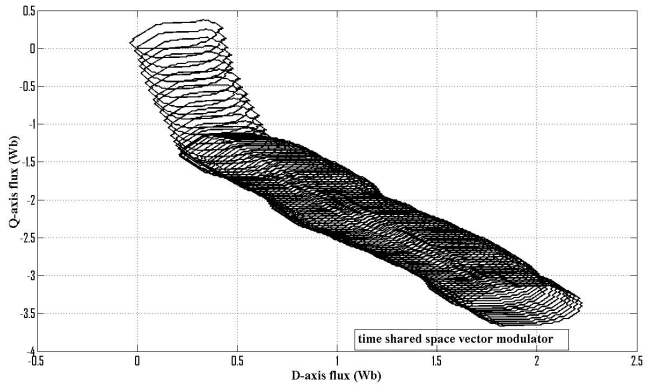

(b)

Fig. 5. Stator flux positions in D-Q axis.

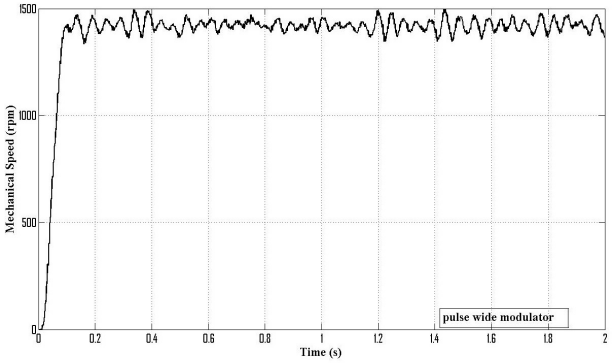

(a)

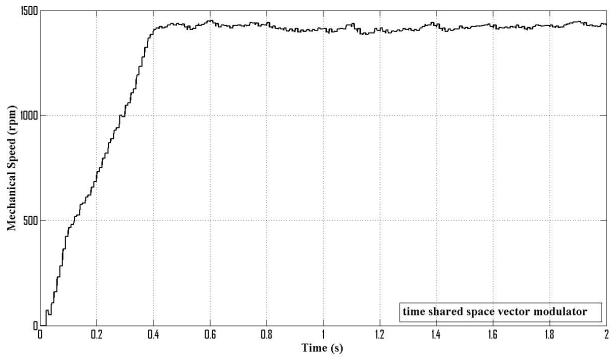

(b)

Fig. 6. Rotor mechanical speed positions.

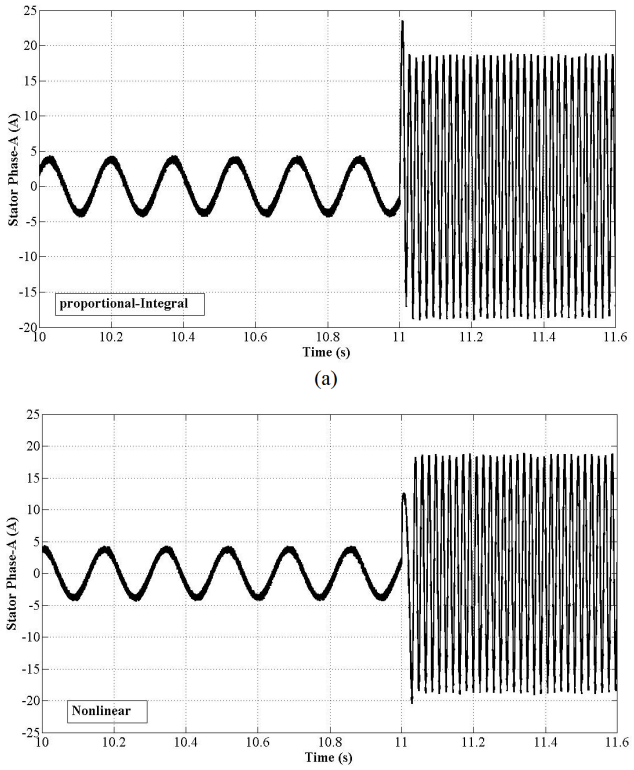

Fig. 7. Stator phase-A current signals time positions.

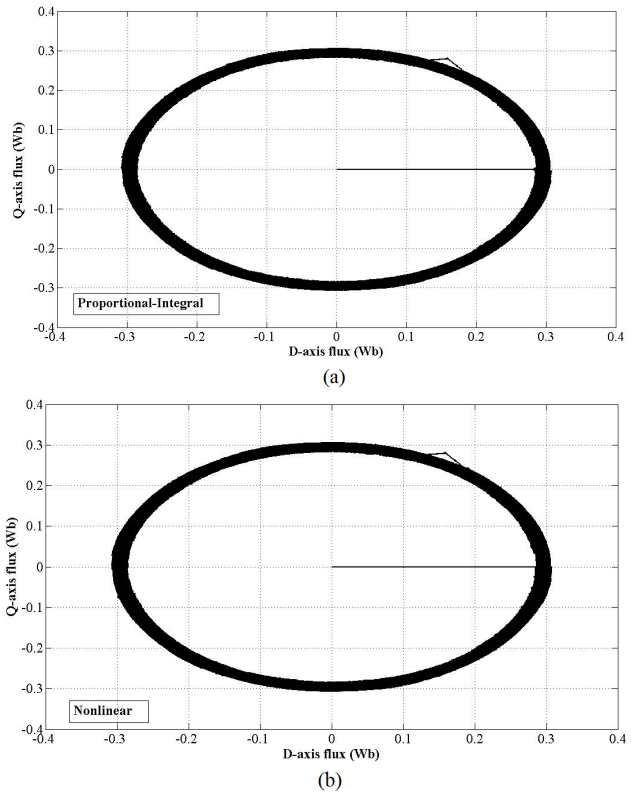

Fig. 8. Stator flux positions in D-Q axis.

To compare the proposed system with classical feedback control and Lyapunov function, 10 μs time constant is used for all discrete time simulations in MATLAB. The same system parameters used in the previous experiments are used. As shown in Fig. 7, stator phase-A currents have nearly same characteristics for both the systems. Also, as shown in Fig. 8, stator flux positions in D-Q axis have nearly same characteristics for both the systems.

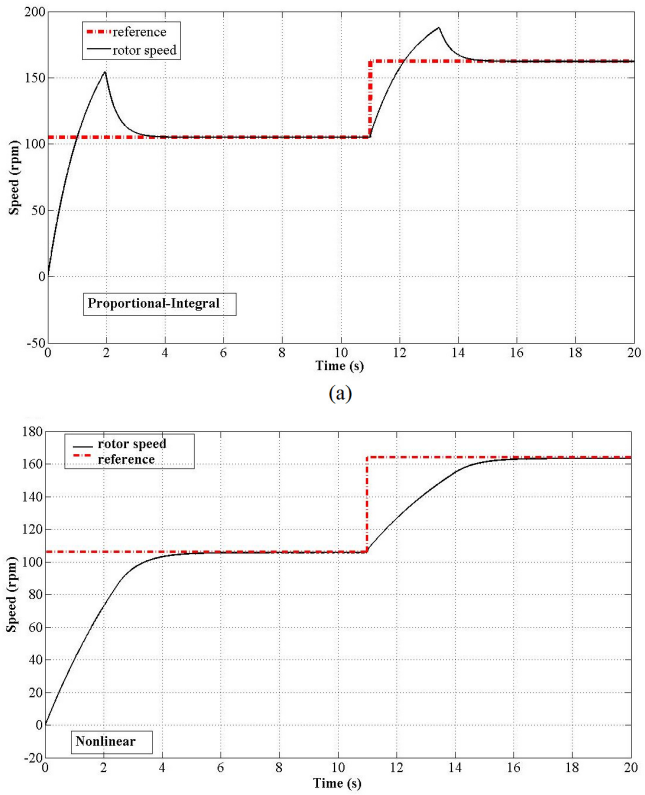

Fig. 9. Rotor mechanical speed positions.

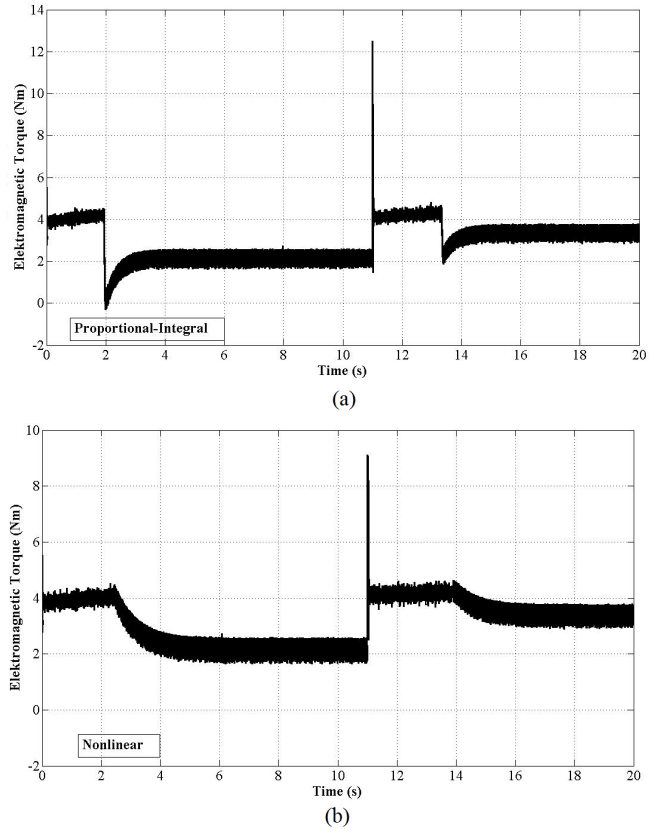

Fig. 10. Stator electromagnetic torque positions in time domain.

As shown in Fig. 9 (a) and (b), the PI controller is 25% faster than the proposed nonlinear controller. However, different from the PI controller, overshoot value of the

proposed controller is zero. In Fig. 10 (a) and (b), stator electromagnetic torque positions in time domain obtained from the PI controller and the proposed nonlinear controller are shown.

V. CONCLUSIONS

In this paper, the details of nonlinear speed controller supported by direct torque control algorithm and space vector modulation are explained. With the results of comparative experimental studies, the performance of the proposed system and its advantages over classical controllers are shown.

Proposed nonlinear speed controller has several advantages over classical controllers such as the use of different Lyapunov functions and easy integration of different system parameters.

REFERENCES

[1] O. Ellabban, J. V. Mierlo, and P. Lataire, "A Comparative Study of Different Control Techniques for an Induction Motor Fed by a Z–Source Inverter for Electric Vehicles", in *Proc. of International Conference on Power Engineering, Energy and Electrical Drives*, Malaga, Spain, 2011, pp. 1–7.

[2] H. Ouadi, F. Giri, A. Elfadili, L. Dugard, "Induction machine speed control with flux optimization", *Control Engineering Practice*, vol. 18, pp. 55–66, 2010. [Online]. Available: http://dx.doi.org/10.1016/j.conengprac.2009.08.006

[3] H. Miranda, P. Cortes, J. I. Yuz, J. Rodriguez, "Predictive Torque Control of Induction Machines Based on State–Space Models", *IEEE Transactions on Industrial Electronics*, vol. 56, no. 6, pp. 1916–1924, 2009. [Online]. Available: http://dx.doi.org/10.1109/TIE.2009.2014904

[4] M. Pucci, "Direct field oriented control of linear induction motors", *Electric Power Systems Research*, vol. 89, pp. 1–7, 2011.

[5] K. Ogata, *Modern Control Engineering.* New Jersey: Prentice Hall, 2002, pp. 53–79.

[6] J. E. Slotine, W. Li, *Applied Non–Linear Control.* New Jersey: Prentice Hall, 1991 pp. 383–453.

[7] H. K. Khalil, *Nonlinear Systems.* New Jersey: Pearson Education, 2000, pp. 87–181.

[8] N. R. N. Idris, A. H. M. Yatim, **"**Direct Torque Control of Induction Machines with Constant Switching Frequency and Reduced Torque Ripple", *IEEE Transactions on Industrial Electronics*, vol. 51, no. 4, pp. 758–767, 2004. [Online]. Available: http://dx.doi.org/10.1109/TIE.2004.831718

[9] P. Vas, *Sensorless Vector and Direct Torque Control.* Oxford: Oxford Science Publications, 1998, pp. 263–352.

[10] H. F. A. Wahab, H. Sanusi, "Simulink Model of Direct Torque Control of Induction Machine", *American Journal of Applied Sciences*, vol. 5, pp. 1083–1090, 2008. [Online]. Available: http://dx.doi.org/10.3844/ajassp.2008.1083.1090

[11] K. Gulez, A. A. Adam, H. Pastaci, "Passive Filter Topology to Minimize Torque Ripples and Harmonic Noises in IPMSM Derived with HDTC", *International Journal of Electronics*, vol. 94, no. 1, pp. 23–33, 2007. [Online]. Available: http://dx.doi.org/10.1080/00207210601070911

[12] C. M. Ong, *Dynamic Simulation of Electric Machinery Using MATLAB/Simulink.* New Jersey: Prentice Hall, 1998, pp. 415–438.

[13] D. Casadei, G. Serre, and K. Tani, "Implementation of a Direct Control Algorithm for Induction Motors Based on Discrete Space Vector Modulation", *IEEE Transactions on Power Electronics*, vol. 15, no. 4, pp. 769–777, 2000. [Online]. Available: http://dx.doi.org/10.1109/63.849048

[14] K. B. Lee and F. Blaabjerg, "Sensorless DTC–SVM for Induction Motor Driven by a Matrix Converter Using a Parameters Estimation Strategy", *IEEE Transactions on Industrial Electronics*, vol. 57, no. 3, pp. 512–521, 2008. [Online]. Available: http://dx.doi.org/10.1109/TIE.2007.911940